

Supplementary Information

This document presents supplementary figures showing bias in the seasonal cycle of precipitation.

Calibration task

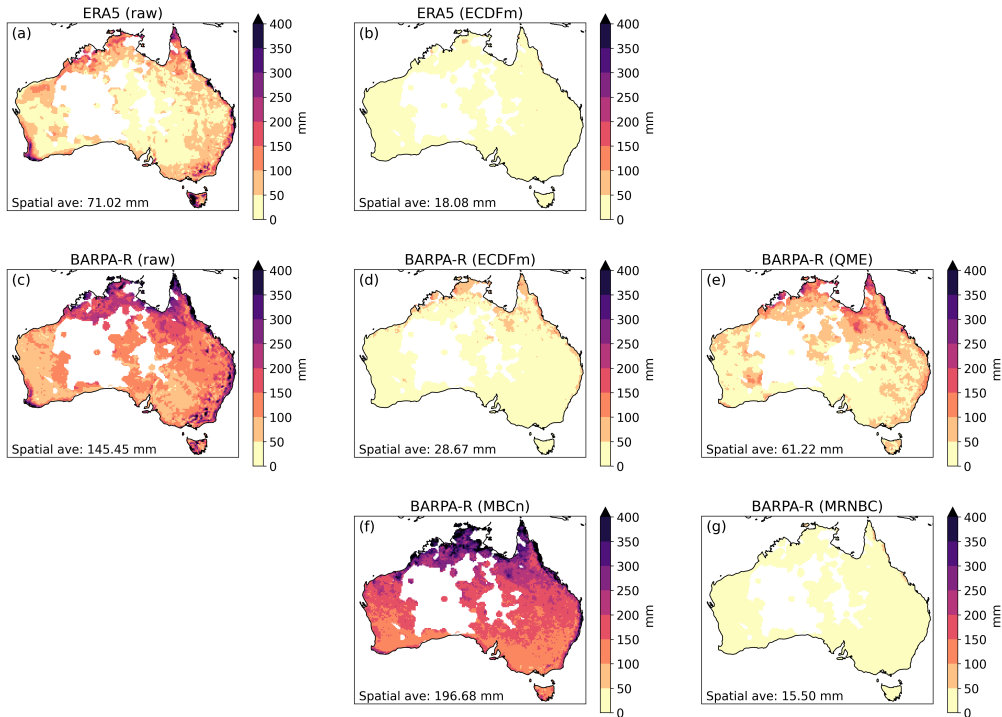


Figure S1: Bias in the seasonal cycle of precipitation (relative to the AGCD dataset) for the calibration assessment task. Results are shown for the ERA5 GCM (panel a), the BARPA-R RCM forced by that GCM (panel c), and various bias correction methods applied to those GCM (panel b) and RCM (panels d-g) data. Land areas where the AGCD data are unreliable due to weather station sparsity have been masked in white.

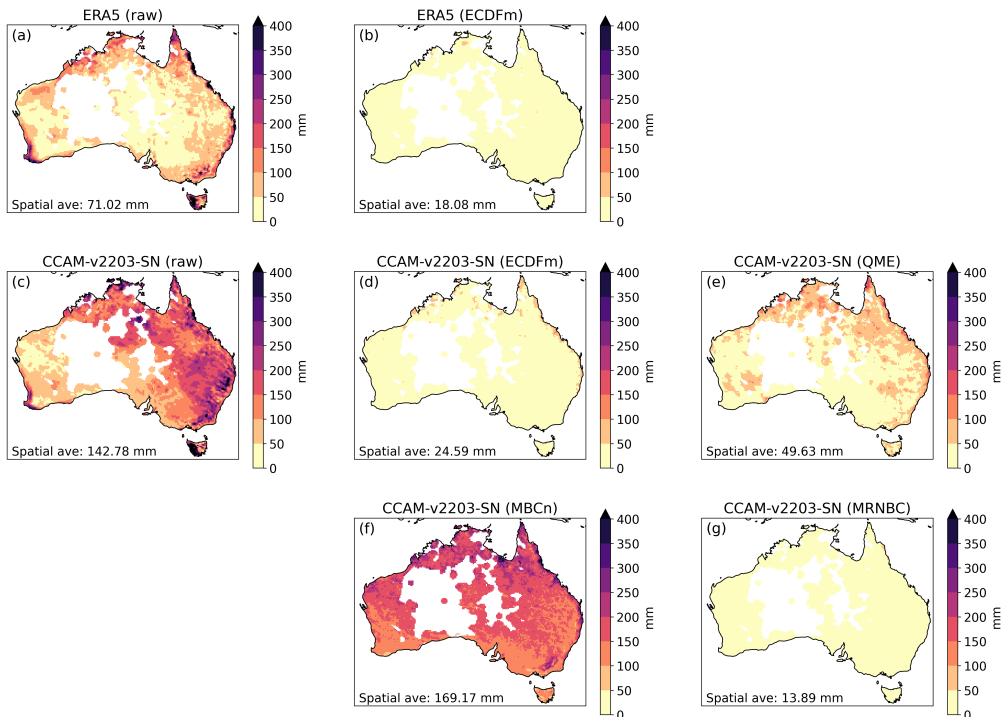


Figure S2: Bias in the seasonal cycle of precipitation (relative to the AGCD dataset) for the calibration assessment task. Results are shown for the ERA5 GCM (panel a), the CCAM-v2203-SN RCM forced by that GCM (panel c), and various bias correction methods applied to those GCM (panel b) and RCM (panels d-g) data. Land areas where the AGCD data are unreliable due to weather station sparsity have been masked in white.

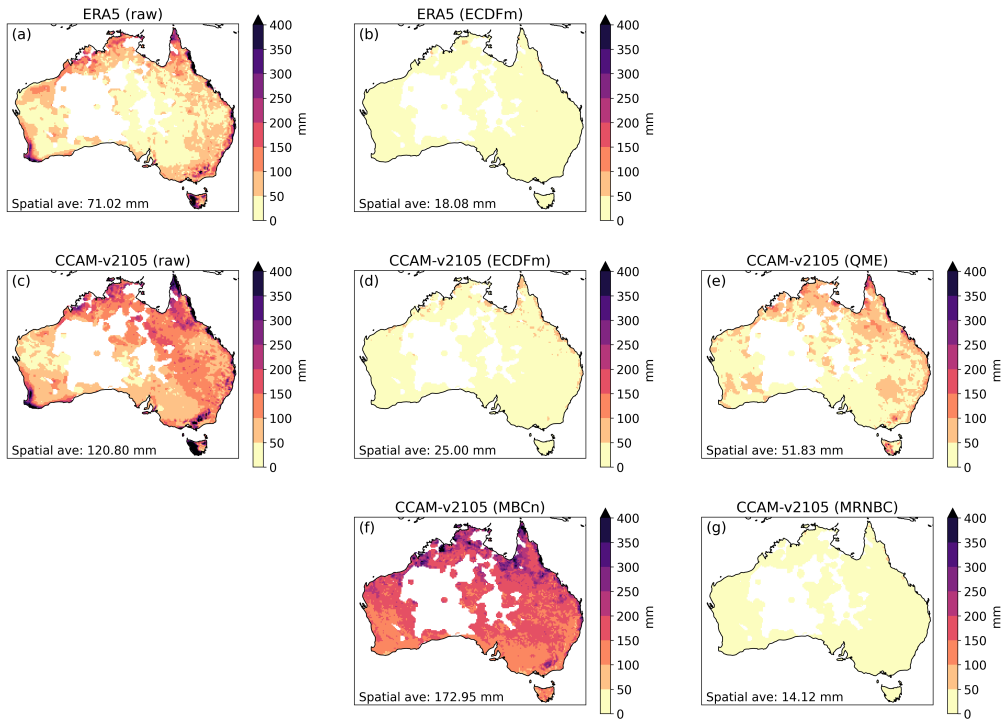


Figure S3: Bias in the seasonal cycle of precipitation (relative to the AGCD dataset) for the calibration assessment task. Results are shown for the ERA5 GCM (panel a), the CCAM-v2105 RCM forced by that GCM (panel c), and various bias correction methods applied to those GCM (panel b) and RCM (panels d-g) data. Land areas where the AGCD data are unreliable due to weather station sparsity have been masked in white.

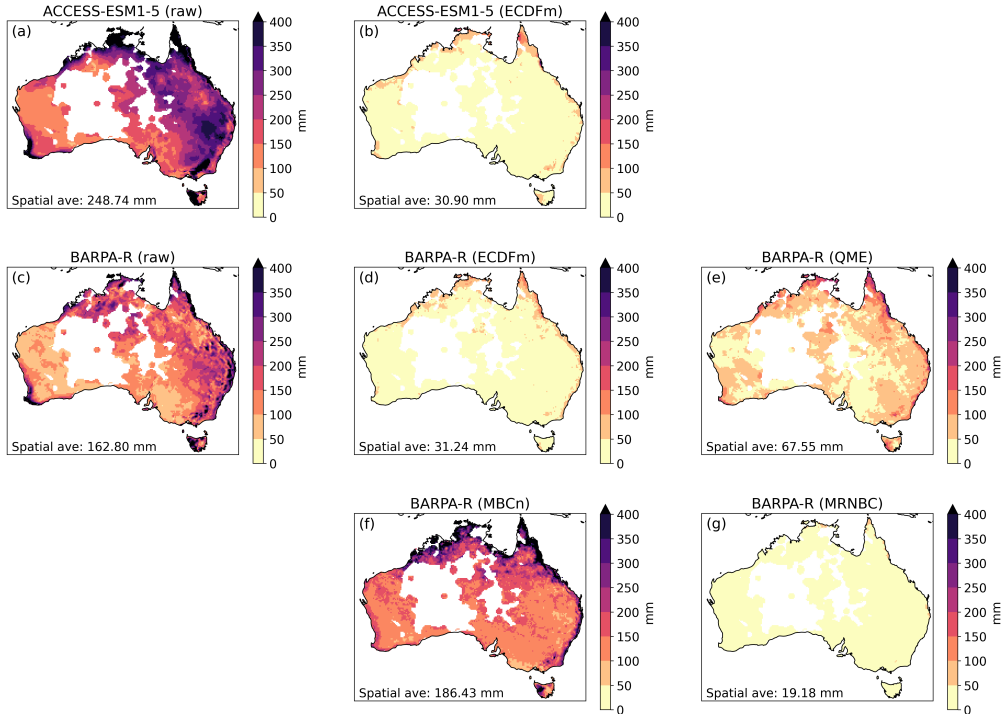


Figure S4: Bias in the seasonal cycle of precipitation (relative to the AGCD dataset) for the calibration assessment task. Results are shown for the ACCESS-ESM1-5 GCM (panel a), the BARPA-R RCM forced by that GCM (panel c), and various bias correction methods applied to those GCM (panel b) and RCM (panels d-g) data. Land areas where the AGCD data are unreliable due to weather station sparsity have been masked in white.

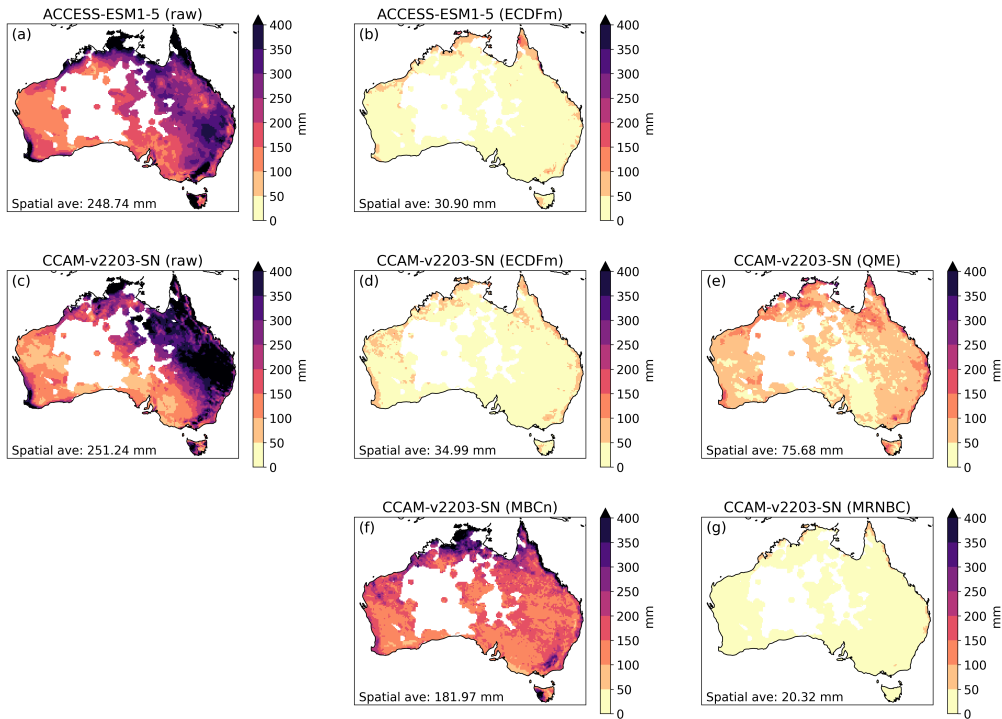


Figure S5: Bias in the seasonal cycle of precipitation (relative to the AGCD dataset) for the calibration assessment task. Results are shown for the ACCESS-ESM1-5 GCM (panel a), the CCAM-v2203-SN RCM forced by that GCM (panel c), and various bias correction methods applied to those GCM (panel b) and RCM (panels d-g) data. Land areas where the AGCD data are unreliable due to weather station sparsity have been masked in white.

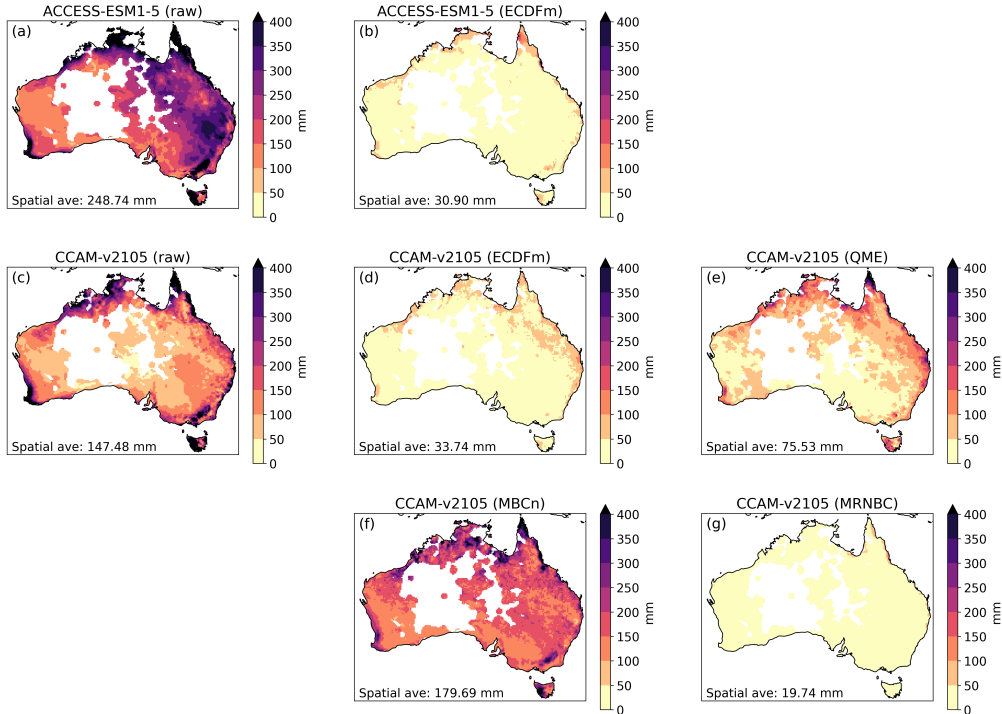


Figure S6: Bias in the seasonal cycle of precipitation (relative to the AGCD dataset) for the calibration assessment task. Results are shown for the ACCESS-ESM1-5 GCM (panel a), the CCAM-v2105 RCM forced by that GCM (panel c), and various bias correction methods applied to those GCM (panel b) and RCM (panels d-g) data. Land areas where the AGCD data are unreliable due to weather station sparsity have been masked in white.

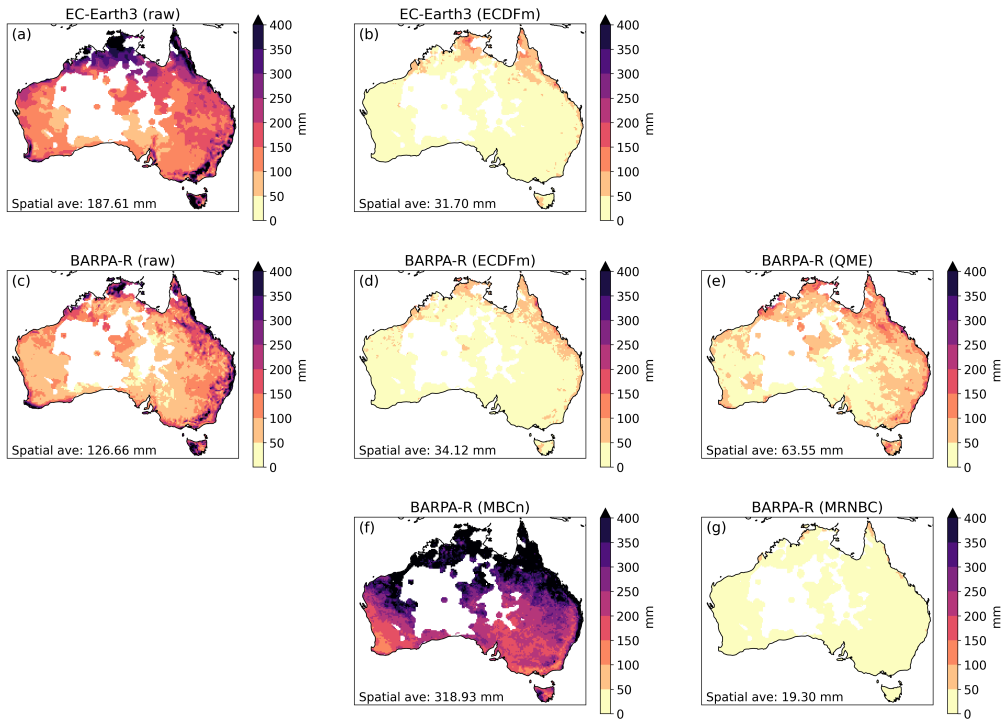


Figure S7: Bias in the seasonal cycle of precipitation (relative to the AGCD dataset) for the calibration assessment task. Results are shown for the EC-Earth3 GCM (panel a), the BARPA-R RCM forced by that GCM (panel c), and various bias correction methods applied to those GCM (panel b) and RCM (panels d-g) data. Land areas where the AGCD data are unreliable due to weather station sparsity have been masked in white.

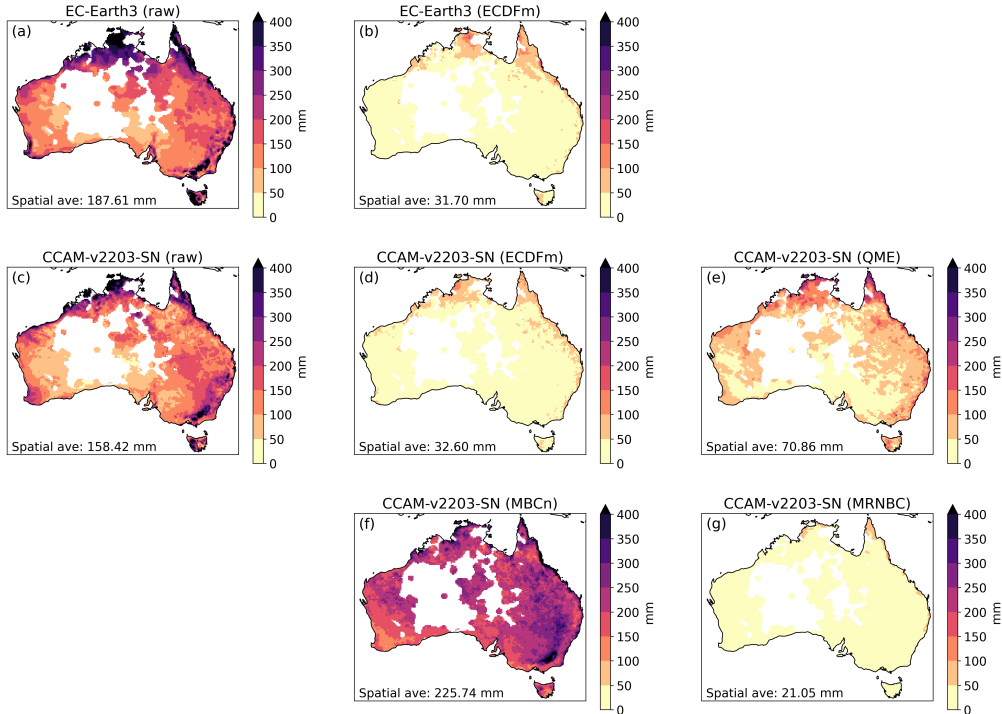


Figure S8: Bias in the seasonal cycle of precipitation (relative to the AGCD dataset) for the calibration assessment task. Results are shown for the EC-Earth3 GCM (panel a), the CCAM-v2203-SN RCM forced by that GCM (panel c), and various bias correction methods applied to those GCM (panel b) and RCM (panels d-g) data. Land areas where the AGCD data are unreliable due to weather station sparsity have been masked in white.

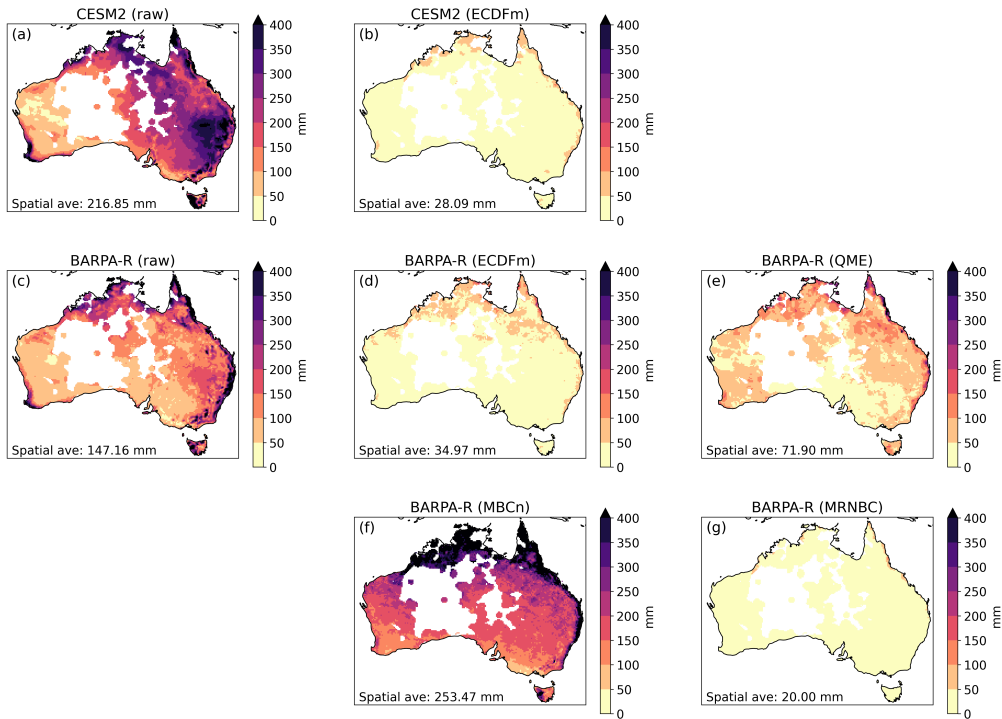


Figure S9: Bias in the seasonal cycle of precipitation (relative to the AGCD dataset) for the calibration assessment task. Results are shown for the CESM2 GCM (panel a), the BARPA-R RCM forced by that GCM (panel c), and various bias correction methods applied to those GCM (panel b) and RCM (panels d-g) data. Land areas where the AGCD data are unreliable due to weather station sparsity have been masked in white.

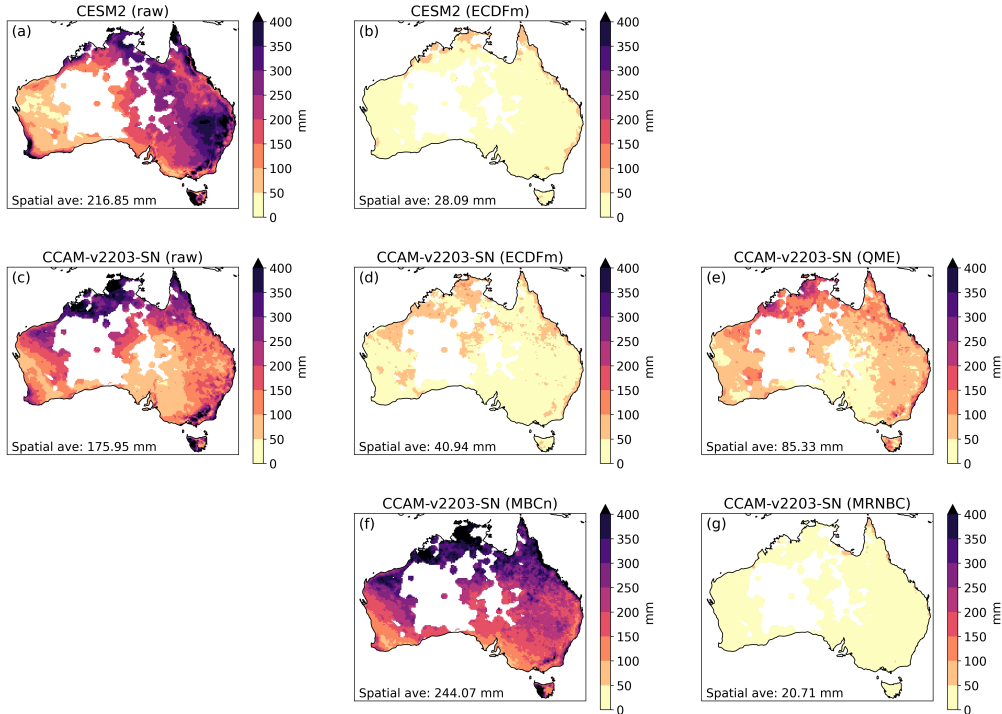


Figure S10: Bias in the seasonal cycle of precipitation (relative to the AGCD dataset) for the calibration assessment task. Results are shown for the CESM2 GCM (panel a), the CCAM-v2203-SN RCM forced by that GCM (panel c), and various bias correction methods applied to those GCM (panel b) and RCM (panels d-g) data. Land areas where the AGCD data are unreliable due to weather station sparsity have been masked in white.

Cross validation task

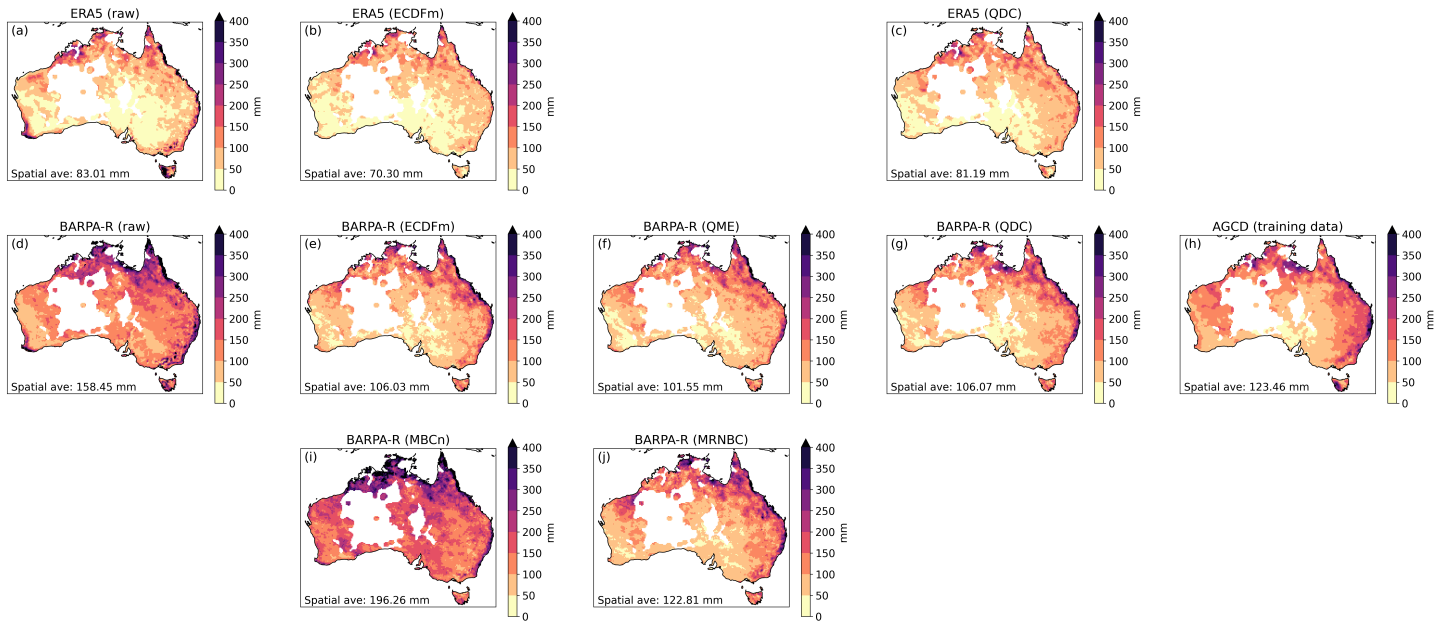


Figure S11: Bias in the seasonal cycle of precipitation (relative to the AGCD dataset) for the cross validation assessment task. Results are shown for the ERA5 GCM (panel a), the BARPA-R RCM forced by that GCM (panel d), and various bias correction methods applied to those GCM (panels b and c) and RCM (panels e, f, g, i and j) data. A reference case where the AGCD training data (1960-1989) was simply duplicated for the assessment period (1990-2019) is also shown (panel h). Land areas where the AGCD data are unreliable due to weather station sparsity have been masked in white.

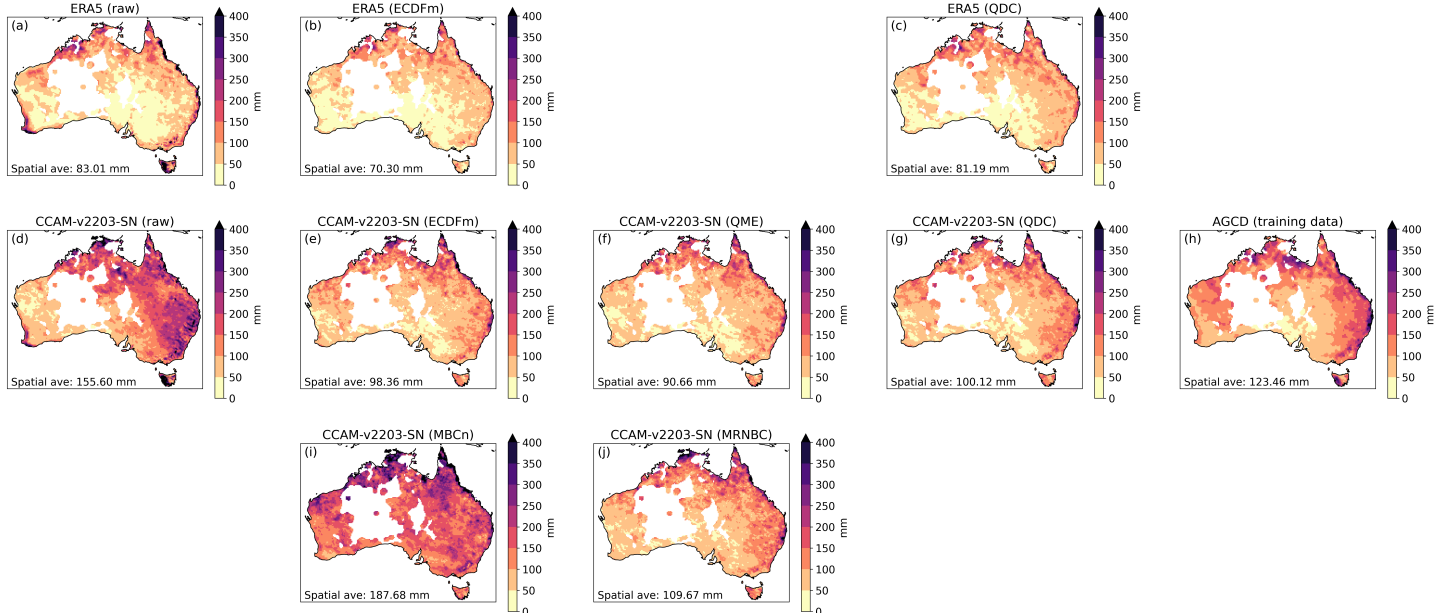


Figure S12: Bias in the seasonal cycle of precipitation (relative to the AGCD dataset) for the cross validation assessment task. Results are shown for the ERA5 GCM (panel a), the CCAM-v2203-SN RCM forced by that GCM (panel d), and various bias correction methods applied to those GCM (panels b and c) and RCM (panels e, f, g, i and j) data. A reference case where the AGCD training data (1960-1989) was simply duplicated for the assessment period (1990-2019) is also shown (panel h). Land areas where the AGCD data are unreliable due to weather station sparsity have been masked in white.

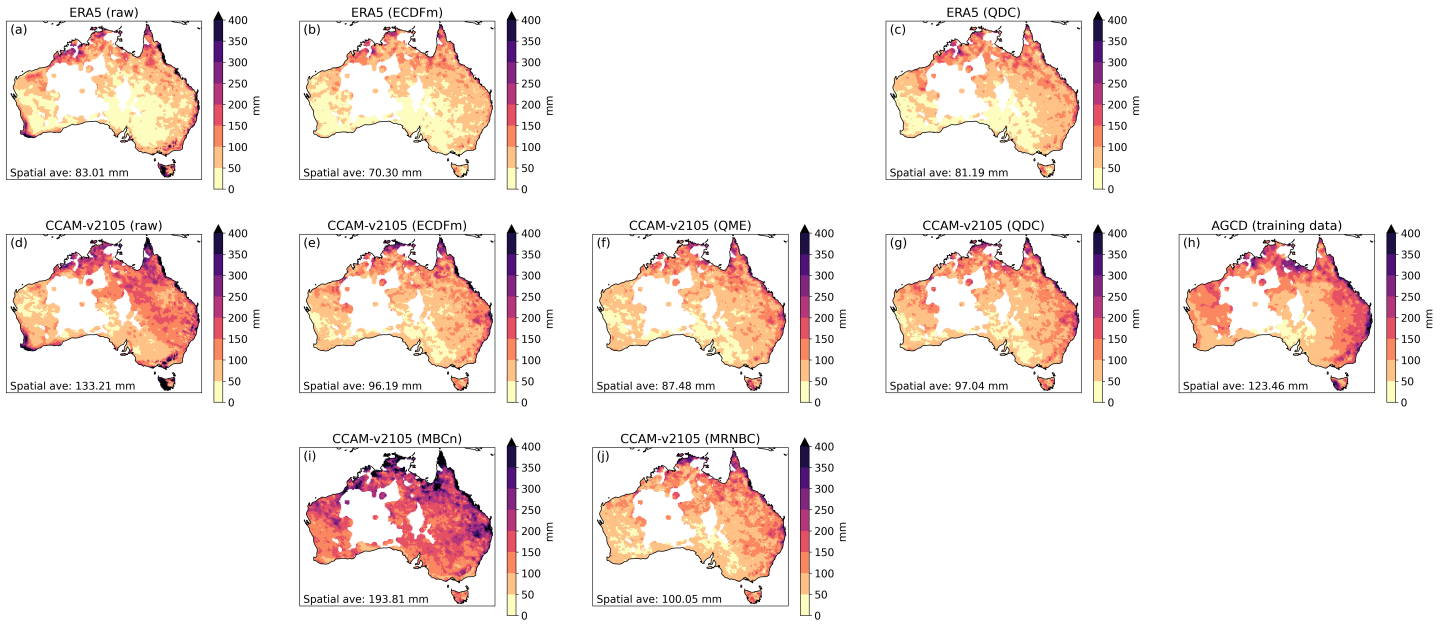


Figure S13: Bias in the seasonal cycle of precipitation (relative to the AGCD dataset) for the cross validation assessment task. Results are shown for the ERA5 GCM (panel a), the CCAM-v2105 RCM forced by that GCM (panel d), and various bias correction methods applied to those GCM (panels b and c) and RCM (panels e, f, g, i and j) data. A reference case where the AGCD training data (1960-1989) was simply duplicated for the assessment period (1990-2019) is also shown (panel h). Land areas where the AGCD data are unreliable due to weather station sparsity have been masked in white.

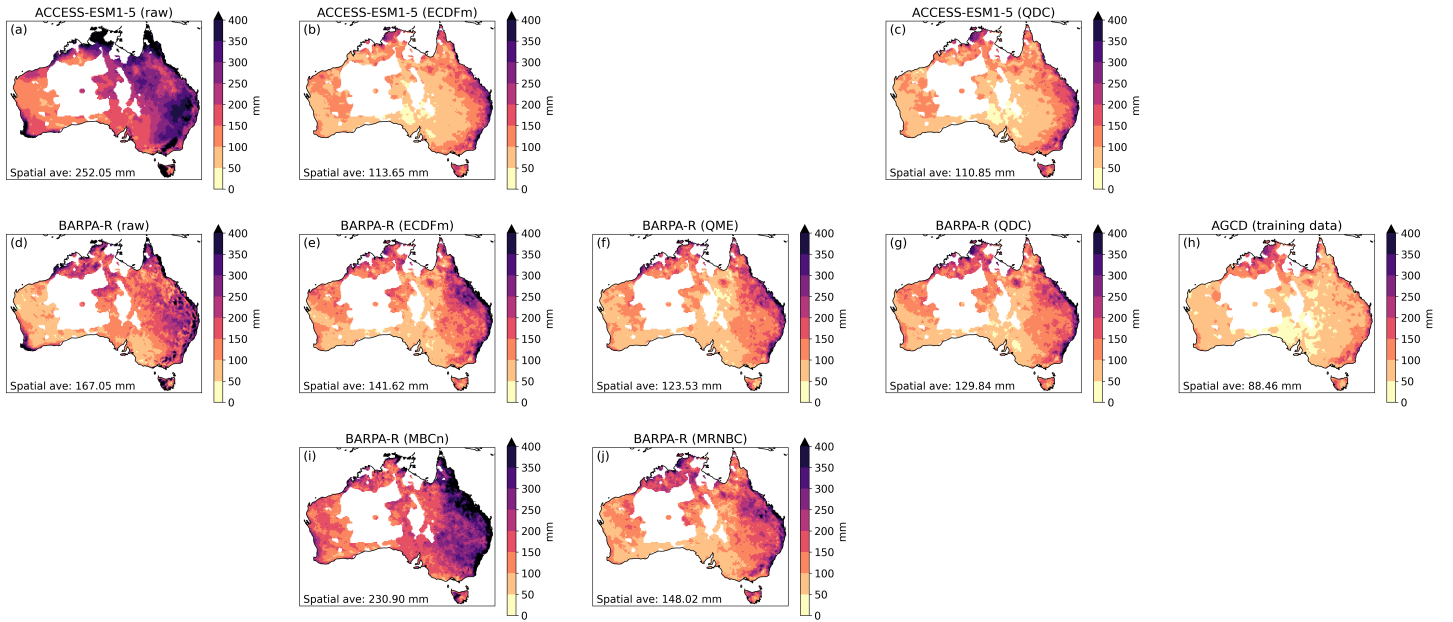


Figure S14: Bias in the seasonal cycle of precipitation (relative to the AGCD dataset) for the cross validation assessment task. Results are shown for the ACCESS-ESM1-5 GCM (panel a), the BARPA-R RCM forced by that GCM (panel d), and various bias correction methods applied to those GCM (panels b and c) and RCM (panels e, f, g, i and j) data. A reference case where the AGCD training data (1960-1989) was simply duplicated for the assessment period (1990-2019) is also shown (panel h). Land areas where the AGCD data are unreliable due to weather station sparsity have been masked in white.

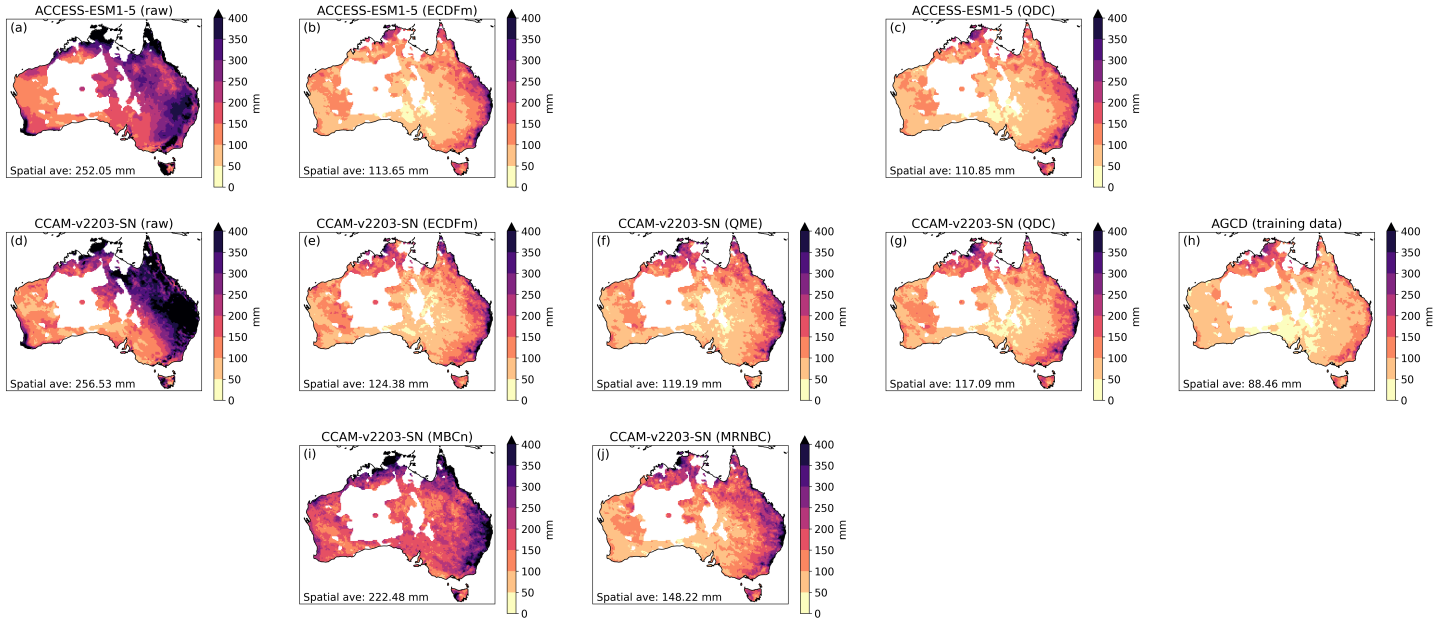


Figure S15: Bias in the seasonal cycle of precipitation (relative to the AGCD dataset) for the cross validation assessment task. Results are shown for the ACCESS-ESM1-5 GCM (panel a), the CCAM-v2203-SN RCM forced by that GCM (panel d), and various bias correction methods applied to those GCM (panels b and c) and RCM (panels e, f, g, i and j) data. A reference case where the AGCD training data (1960-1989) was simply duplicated for the assessment period (1990-2019) is also shown (panel h). Land areas where the AGCD data are unreliable due to weather station sparsity have been masked in white.

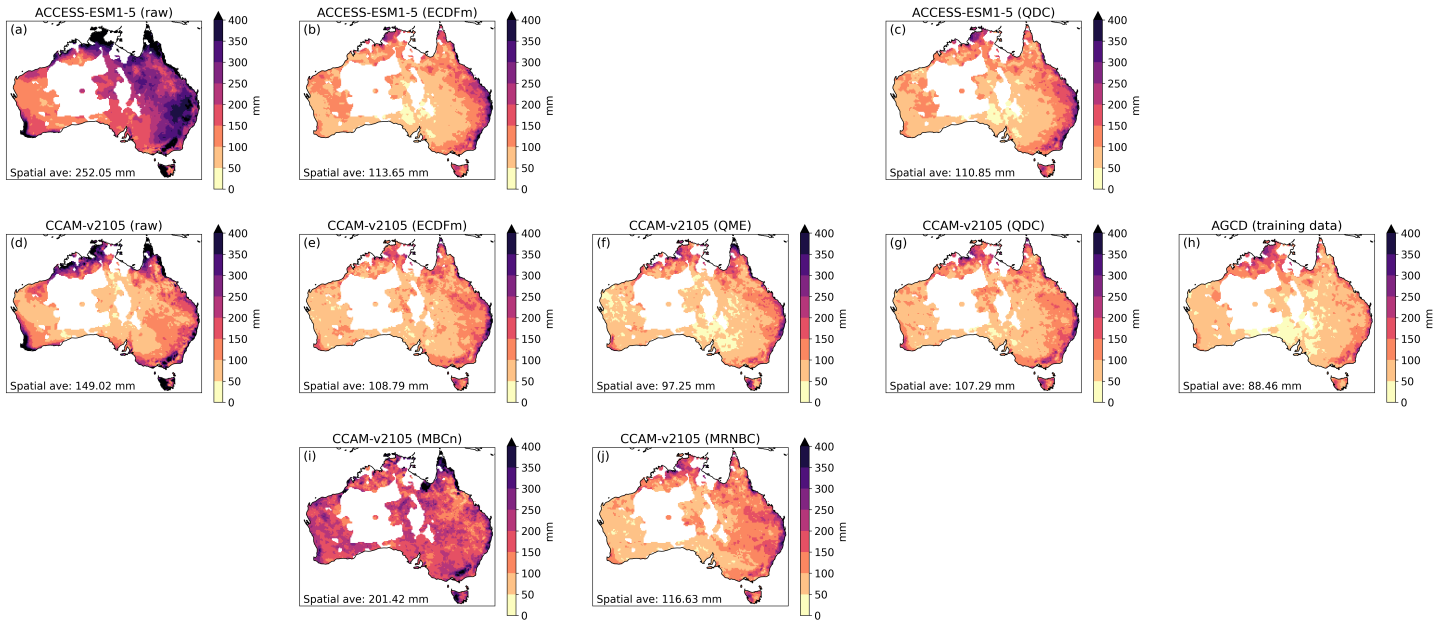


Figure S16: Bias in the seasonal cycle of precipitation (relative to the AGCD dataset) for the cross validation assessment task. Results are shown for the ACCESS-ESM1-5 GCM (panel a), the CCAM-v2105 RCM forced by that GCM (panel d), and various bias correction methods applied to those GCM (panels b and c) and RCM (panels e, f, g, i and j) data. A reference case where the AGCD training data (1960-1989) was simply duplicated for the assessment period (1990-2019) is also shown (panel h). Land areas where the AGCD data are unreliable due to weather station sparsity have been masked in white.

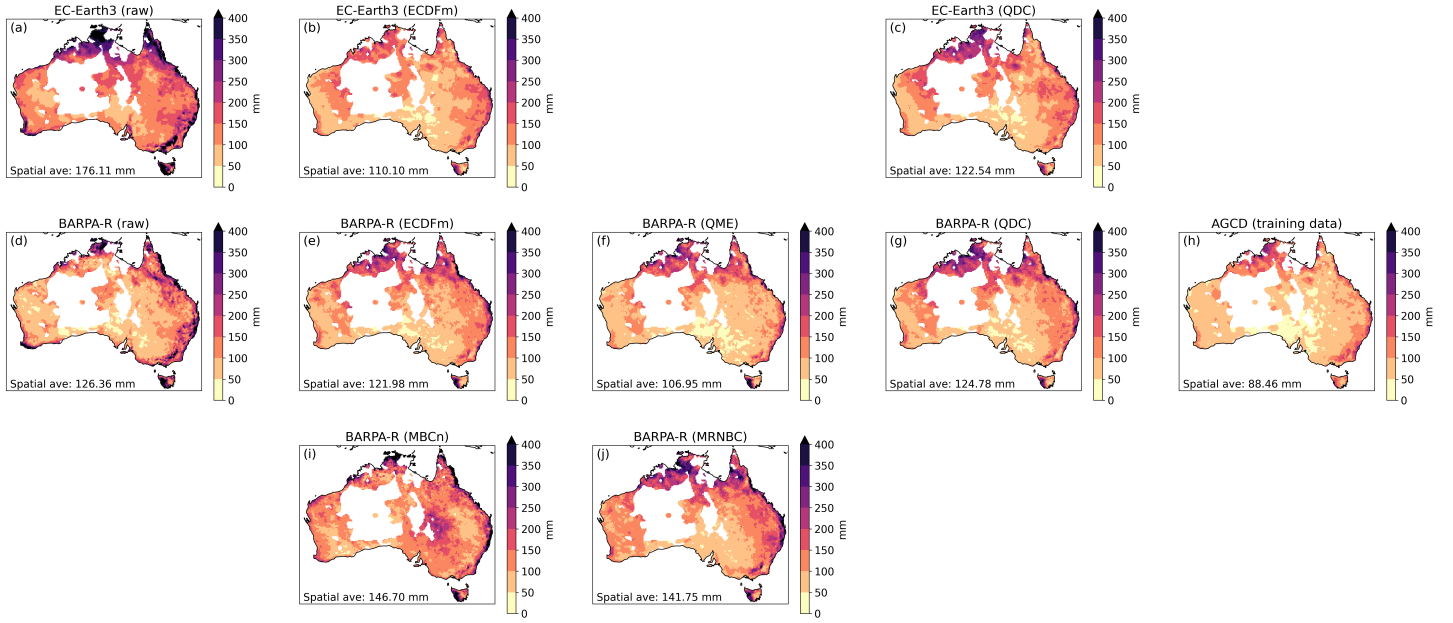


Figure S17: Bias in the seasonal cycle of precipitation (relative to the AGCD dataset) for the cross validation assessment task. Results are shown for the EC-Earth3 GCM (panel a), the BARPA-R RCM forced by that GCM (panel d), and various bias correction methods applied to those GCM (panels b and c) and RCM (panels e, f, g, i and j) data. A reference case where the AGCD training data (1960-1989) was simply duplicated for the assessment period (1990-2019) is also shown (panel h). Land areas where the AGCD data are unreliable due to weather station sparsity have been masked in white.

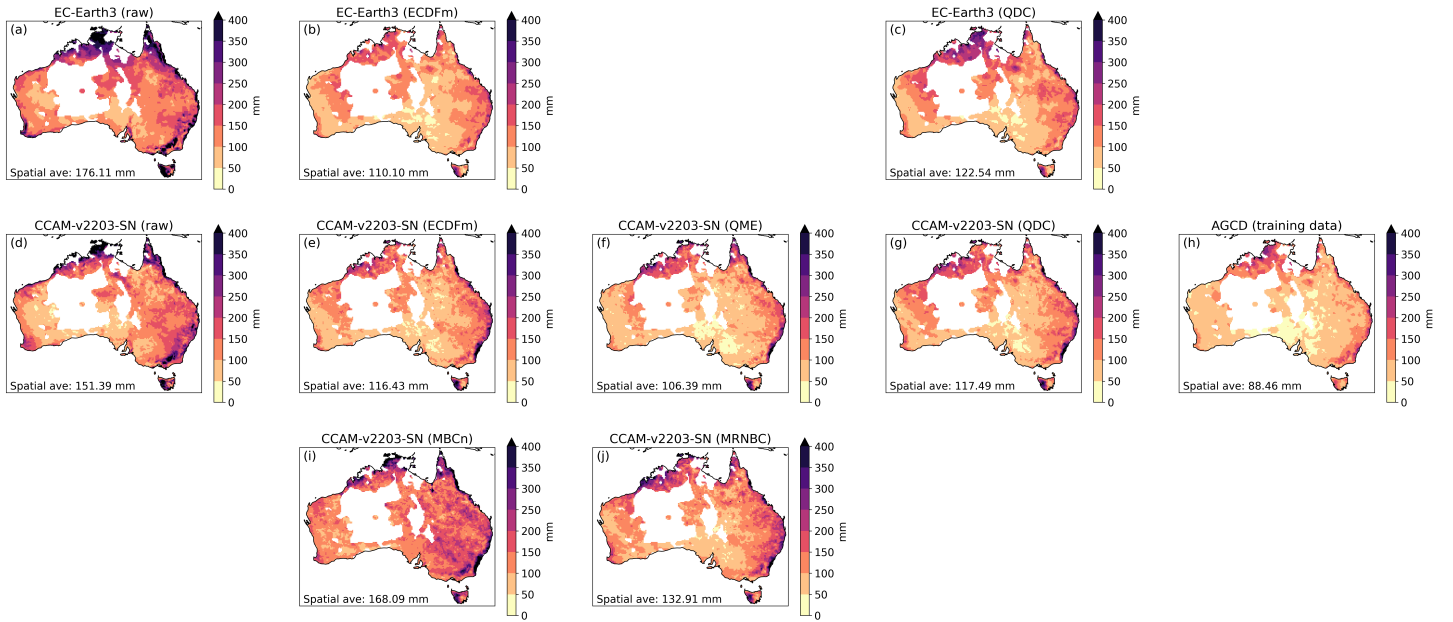


Figure S18: Bias in the seasonal cycle of precipitation (relative to the AGCD dataset) for the cross validation assessment task. Results are shown for the EC-Earth3 GCM (panel a), the CCAM-v2203-SN RCM forced by that GCM (panel d), and various bias correction methods applied to those GCM (panels b and c) and RCM (panels e, f, g, i and j) data. A reference case where the AGCD training data (1960-1989) was simply duplicated for the assessment period (1990-2019) is also shown (panel h). Land areas where the AGCD data are unreliable due to weather station sparsity have been masked in white.

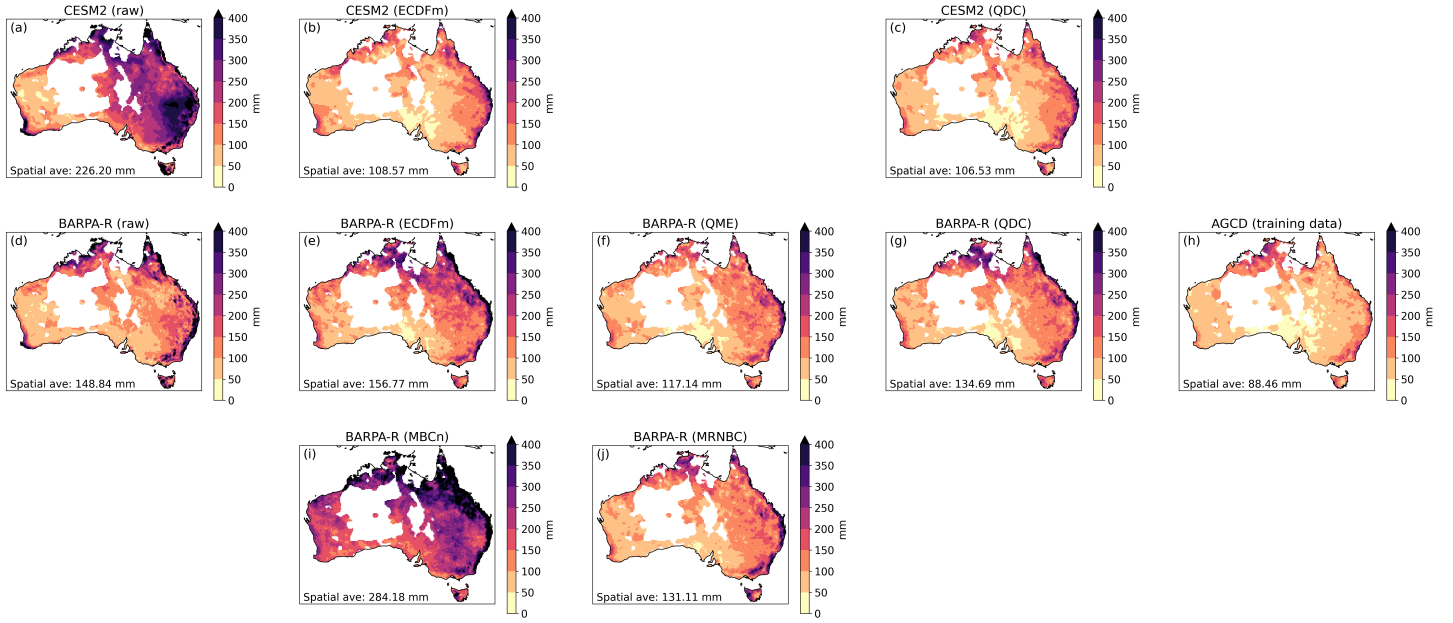


Figure S19: Bias in the seasonal cycle of precipitation (relative to the AGCD dataset) for the cross validation assessment task. Results are shown for the CESM2 GCM (panel a), the BARPA-R RCM forced by that GCM (panel d), and various bias correction methods applied to those GCM (panels b and c) and RCM (panels e, f, g, i and j) data. A reference case where the AGCD training data (1960–1989) was simply duplicated for the assessment period (1990–2019) is also shown (panel h). Land areas where the AGCD data are unreliable due to weather station sparsity have been masked in white.

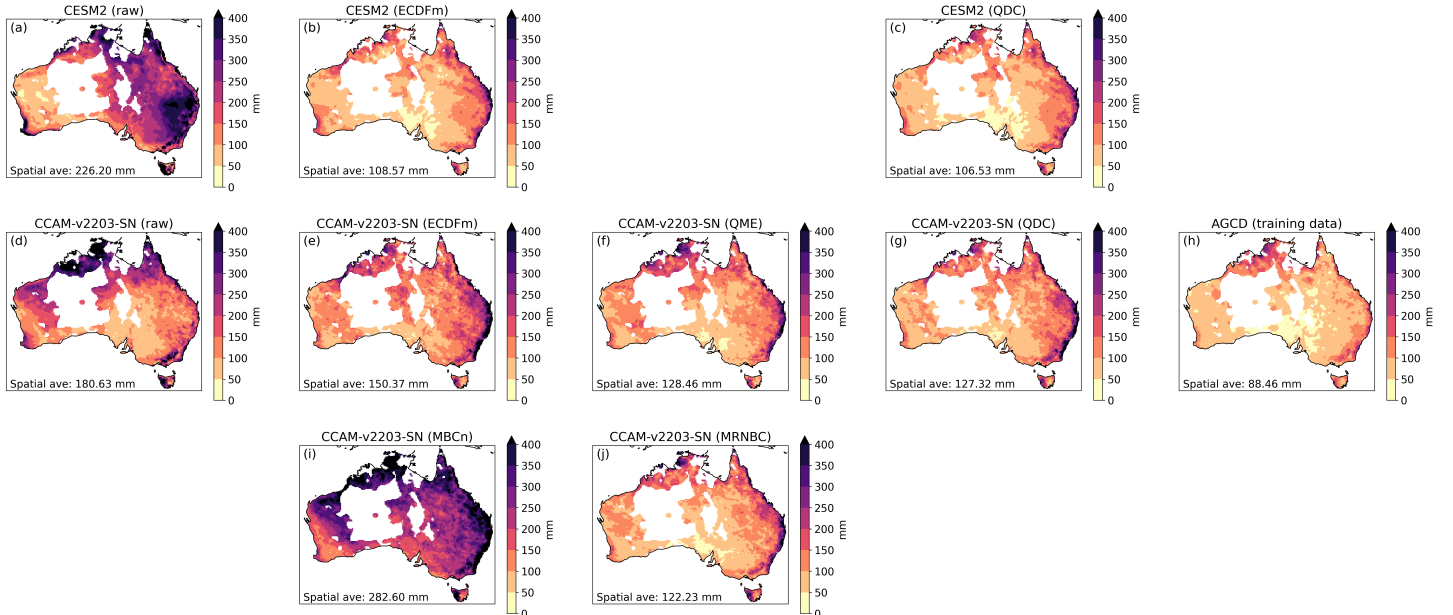


Figure S20: Bias in the seasonal cycle of precipitation (relative to the AGCD dataset) for the cross validation assessment task. Results are shown for the CESM2 GCM (panel a), the CCAM-v2203-SN RCM forced by that GCM (panel d), and various bias correction methods applied to those GCM (panels b and c) and RCM (panels e, f, g, i and j) data. A reference case where the AGCD training data (1960–1989) was simply duplicated for the assessment period (1990–2019) is also shown (panel h). Land areas where the AGCD data are unreliable due to weather station sparsity have been masked in white.